Journal of Applied Polymer Science

Feasibility of recycled newspaper as cellulose source for regenerated cellulose membrane fabrication

Mohamad Azuwa Mohamed,[1,2] W. N. W. Salleh,[1,2] Juhana Jaafar,[1,2] A. F. Ismail,[1,2] Muhazri Abd. Mutalib,[1,2] Siti Munira Jamil[1,2]

[1]Advanced Membrane Technology Research Centre, Universiti Teknologi Malaysia, 81310 Skudai, Johor Bahru, Malaysia
[2]Faculty of Petroleum and Renewable Energy Engineering, Universiti Teknologi Malaysia, 81310 Skudai, Johor Bahru, Malaysia
Correspondence to: W. N. W. Salleh (E-mail: hayati@petroleum.utm.my)

ABSTRACT: An environmental friendly regenerated cellulose membrane (RCM) was successfully prepared via NaOH/urea aqueous solution system by utilizing recycled newspaper (RNP) as the cellulose source. The morphological and chemical structure of resulting membrane were characterized using scanning electron microscopy (SEM), atomic force microscopy (AFM), transmission electron microscopy (TEM), Fourier transform infrared (FTIR) spectroscopy, X-ray diffraction (XRD) spectroscopy, and thermogravimetric analysis (TGA). Results from FTIR and XRD verified that the transparent RCM possesses cellulose II structure. SEM observation revealed that the transparent RCM consist of homogeneous dense symmetric membrane structure and composed of a skin layer with mean roughness parameter R_a, obtained from AFM analysis of 29.53 nm. Pure water flux, water content, water contact angle, porosity, and pore size of the resulting membrane were also measured. This study promotes the potential of the cellulose-based membrane obtained from low cost cellulose source for application in filtration and separation system. © 2015 Wiley Periodicals, Inc. J. Appl. Polym. Sci. **2015**, *132*, 42684.

KEYWORDS: biopolymers and renewable polymers; cellulose and other wood products; membranes; morphology; recycling

Received 21 April 2015; accepted 30 June 2015
DOI: 10.1002/app.42684

INTRODUCTION

The rapid developments in synthetic polymer have provided great benefits to the modern society. However, the waste from synthetic polymer is difficult to degrade and dispose of, resulting in severe urban environmental consequences. As environmental sustainability is concerned, the world is in urged to search for an alternative source in order to prevent and control the white pollutions. The white pollutions will lead to the detrimental effects on soil structure, water and nutrient transport, and crop growth, thereby disrupting the agricultural environment and reducing crop production.[1] Among the alternatives, polymer recycling and returning to biologically based renewable polymers may be emphasized.[2,3] Cellulose is unquestionably the most abundant naturally occurring reproducible organic compound and it will become the main chemical resource in the future.[4]

Regenerated cellulose membrane (RCM) has been extensively commercialized in the field of membrane science and technology involving various membrane separation processes, such as microfiltration, ultrafiltration, nanofiltration, reverse osmosis, gas separation, and pervaporation.[5–12] Moreover, the regenerated cellulose can be a promising biobased packaging materials as well as for wound dressing.[8,13,14] The versatility of cellulose to be applied in various applications is due to its low cost, strong hydrophilicity properties, fascinating structure, biocompatibility, and derivable properties.[15,16] In recent years, the green comprehensive utilization of cellulose resources has drawn much attention from governments and researchers.[3] Previous studies have utilized various sources of cellulose in the fabrication of RCM such as cotton linter, soft wood pulp, and microcrystalline cellulose.[17–19] To the best of our knowledge, there is yet any research attempt of preparing RCM by utilizing old recycled newspaper (RNP) as a cellulose sources. This would be an environmental friendly approach since tonnes of newspapers are discarded every year. Therefore, it is important to assess the feasibility of old RNP as the cellulose sources for the preparation of environmental friendly RCM.

Recently, a variety of solvents based on aqueous alkali (containing NaOH and urea) have been developed and shown to be suitable for fiber spinning, membrane and aerogel formation, cellulose blending, and homogeneous cellulose modification.[20] A number of researchers reported that the 7 wt % NaOH/12 wt % urea aqueous solution pre-cooled to −12°C has been

developed as low cost solvent for rapid dissolution of cellulose.[3,21–25] It have been proven that the presence of NaOH hydrates and urea hydrates in the aqueous solution is the key for the cellulose dissolution at low temperature.[26] The main advantages of this solvent system are its rapid dissolution, ease of handling, economy, and environmental friendly material.

In this study, we prepared a RCM by utilizing old newspaper to obtain the cellulose, in which the dissolution of the cellulose was carried out via pre-cooled 7 wt % NaOH/ 12 wt % urea aqueous solution system. Scanning electron microscopy (SEM), atomic force microscopy (AFM), transmission electron microscopy (TEM), Fourier transform infrared (FTIR) spectroscopy, X-ray diffraction (XRD) spectroscopy, and thermal gravimetric analysis (TGA) were carried out to investigate the physicochemical and structural properties of the RCM. In addition, the physical characteristics of resulting membrane were studied in terms of pure water flux, water content (WC), water contact angle, porosity, and pore size. The fabrication of RCM by utilizing RNP can promote a truly 'green' method for the preparation of RCM in terms of dissolving process and cost-effective recycled cellulose-based materials.

EXPERIMENTAL

Materials

Non-printed area of the RNP was used as the raw material for cellulose source. Sodium hydroxide (NaOH) pallets, sulphuric acid (H_2SO_4) (95–97%), and nitric acid (HNO_3) (65%) were purchased from QReC Malaysia. Sodium chlorite ($NaClO_2$) (80%) was purchased from Sigma Aldrich. All of the chemicals were of reagent grade and used as received.

Extraction of Cellulose

Cellulose was extracted according to our previous study,[27] which is described below: Non-printed area of the RNP was ground until its fibrous strand was obtained, and then dried in oven at 50°C for 24 h. The ground RNP was treated with 5 wt % of NaOH at 100°C for 4 h. The ratio between ground RNP and NaOH solution was 1 : 40 (g/mL). Subsequently, bleaching treatment was carried out using $NaClO_2$ solutions. About few drops of 60 wt % HNO_3 were added dropwise into 800 mL 2 w/v % of $NaClO_2$ solution at 100°C under vigorous mechanical stirring. After that, the sample was immediately added into $NaClO_2$ solution and boiled at 100°C for 4 h under continuous vigorous mechanical stirring. After each step of alkali and bleaching treatment, the sample was washed with running tap water and finally washed with distilled water until neutral pH was achieved. The sample was then dried in the oven at 50°C for 24 h.

Preparation of Regenerated Cellulose Membrane

To prepare the membrane, an aqueous solution consisting of 7 wt % NaOH/12 wt % urea was prepared and the solution was pre-cooled to −15°C. A desired amount of cellulose was immediately dispersed into the pre-cooled aqueous solution under continuous vigorous mechanical stirring until 4 wt % of cellulose dope was obtained. The resulting cellulose dope was then subjected to centrifugation to eliminate the air bubbles and to discard the remaining undissolved portion, at 4000 rpm for 1 h. The transparent cellulose dope solution was casted on a glass plate and immediately immersed in 5 wt % of H_2SO_4 coagulant bath for 10 min. After the membrane was detached from the glass plate, the wet membrane was washed with running tap water and finally washed with distilled water to remove excess H_2SO_4 on the surface of the prepared membrane. Finally, the wet membrane was transferred onto a glass plate and dried at room temperature of 25°C.

CHARACTERIZATION METHODS

Morphological Analysis

The surface and cross sectional morphology was examined by using SEM, brand TM-3000 Hitachi at an acceleration voltage 15 kV. The samples were sputter coated with platinum to avoid charging. The pore size distributions of the samples were studied by using an AFM. AFM measurement was performed using an atomic force microscope (XE-100 Park System) with SSS-NCHR non-contact probes at 1 μm/s of scan speed. Transmission electron microscopy was carried out using (TEM) PHILPS CM12 at an accelerating voltage of 100 kV.

Fourier Transforms Infrared Spectroscopy

FT-IR spectra were carried out on a Perkin Elmer infrared spectrometer using attenuated total reflection (ATR) accessory to provide non-destructive measurement method. All samples were directly put in contact with ATR diamond by clamping each sample onto the diamond surface, and then pressure was applied to ensure good optical contact between the sample and the diamond. All samples were scanned within the wave range of 650–4000 cm^{-1} at room temperature with relative humidity of 40–50% and instrument resolution is about 0.5 cm^{-1} to 64 cm^{-1}.

X-ray Diffraction

The crystallinity of samples was determined by using Siemens X-ray diffractometer D5000 with CuKα radiation of wavelength 0.15406 nm at 40 kV and 40 mA. The diffracted intensity was measured within scan range $2\theta = 5–80°$ with a step speed of 2° min^{-1}. The crystallinity of the samples was calculated from the diffraction intensity data using the empirical method for native cellulose. The crystalline-to-amorphous ratio material was determined using eq. (1).

$$C_r.I\ (\%) = \frac{I_{002} - I_{am}}{I_{002}} \quad (1)$$

where C_rI is the crystallinity index, I_{oo2} is the maximum intensity (in arbitrary units) of the diffraction from 002 plane at $2\theta = 22.6°$, and I_{am} is the intensity of the background scatter measured at $2\theta = 19°$.[28]

Thermogravimetric Analysis

Thermal stability was characterized using thermogravimetry analyzer (Mettler Toledo). Dry sample was ground into fine powder and then placed in a platinum pan with the heating rate of 10°C min^{-1} over 20–600°C temperature range under nitrogen atmosphere, with a nitrogen flow rate of 20 mL min^{-1}.

Water Content and Contact Angle Analysis

The water contact angle of the RCM was determined by using a contact angle goniometer (OCA15Pro, Data Physics), equipped with image-processing software. This tool was used to evaluate the degree of membrane hydrophilicity via sessile drop

technique. Five contact angle measurements were performed for each sample, whose average and the standard deviation were calculated.

WC was obtained by the immersion of the dried film in water for 24 h at room temperature. The wet film was then removed from water and the excess water on the surface of the film was removed by mopping it with blotting paper. The weight of the wet film was measured, and it was placed in vacuum oven at 70°C for 48 h. The weight of dry film was measured and the WC was calculated with the following equation:[29]

$$\mathrm{WC}\% = \frac{W_w - W_d}{W_w} \times 100 \quad (2)$$

where W_w and W_d are the weight of wet and dry membrane (g), respectively.

Pure Water Flux

The pure water flux (J) of film samples were measured using water permeability equipment at 2.0 bar pressure feed pressure and room temperature as shown in Figure 1. In order to minimize concentration polarization during the experiment, Teflon-coated magnetic stirring bar was used and controlled at 1200 rpm on top of the active side of membrane. Membrane circular coupons were of 14.6 cm^2 (effective diameter: 4.3 cm). The newly prepared RCM membranes were pre-pressured to minimize their compaction effects using deionized water for 30 min at 3.0 bar pressure before measurement. The pure water flux (J) was calculated by using the following equation:

$$J = \frac{V}{A.t} \quad (3)$$

where J is the pure water flux, V is the permeated volume water (mL), t is the permeation time (h), and A is the membrane area (14.6 cm^2).

Membrane Porosity

The porosity of the prepared films was determined via gravimetric method as expressed in the following equation:[30]

$$\varepsilon(\%) = \frac{\frac{(W_w - W_d)}{\rho_H}}{\frac{(W_w - W_d)}{\rho_H} + \frac{W_d}{\rho_c}} \quad (4)$$

where W_w and W_d are the weight of wet and dry membrane (g), respectively. ρ_H is the density of water (0.998 g/cm^3), and ρ_c is the density of cellulose (1.5 g/cm^3).

Membrane Mean Pore Size

The mean pore radius, r_f was calculated by employing the following equation, derived based on the straight through cylindrical pore model:[18]

$$r_f = \sqrt{\frac{8 \times \eta \times l \times J}{\varepsilon \times \Delta P}} \quad (5)$$

where η is the water viscosity (8.9×10^{-4} Pa s), l is the membrane thickness (m), J is the permeation flux (m^3 m^{-2} s^{-1}), and ΔP is the load pressure (Pa).

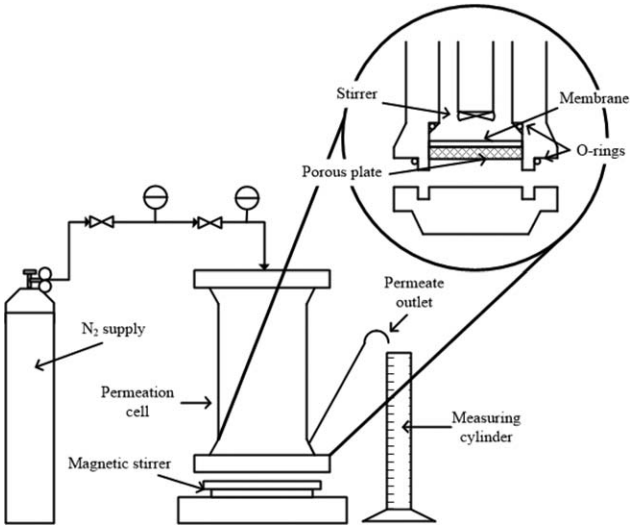

Figure 1. Schematic diagram of dead-end permeation cell.

RESULTS AND DISCUSSION

Morphological Analysis

The extraction of the cellulose microfiber resulted in morphological changes, as well as chemical changes on the cellulose microfiber surfaces. SEM images of the recycled newspaper (RNP-pulp) and treated cellulose microfibers (t-CMF) are shown in Figure 2(a,b). It was observed that the structure of cellulose chain became smoother and had cleaner surface, which indicated the removal of lignin, with some others extractives surrounding the fiber via NaOH pretreatment and delignification with acidified $NaClO_2$. Similar observation was also been reported in previous study.[31] It was revealed that an average diameter of the t-CMF decreased from the original RNP-pulp from 12 to 15 μm to 5–8 μm. The decrease in average diameter exhibited the production of highly purified cellulose microfibers.[27] In addition, the extraction of the cellulose microfiber from RNP-pulp produced white colored treated cellulose powder, as shown in Figure 2(c). This white powder was further used for the preparation of cellulose dope solution. Figure 2(d) shows a photograph of the transparent cellulose dope solution obtained from preparation technique using 7 wt % NaOH/12 wt % urea aqueous solutions and pre-cooled to −15°C. Cellulose is not soluble in usual solvent due to strong inter and intramolecular hydrogen bonds. Nevertheless, previous studies have shown that RCM can be produced from this cellulose dope solution.[12,17,32]

Figure 3(a,d) shows the SEM images of the RCM surface and cross section, respectively. The SEM images revealed that, the transparent cellulose membrane presented smooth surface, while the cross sectional image confirmed that the prepared cellulose membrane acquired homogeneous dense symmetric membrane structure which composed of a skin layer. The formation of the skin layer results from the increase in polymer concentration stimulated by an extremely rapid solvent depletion from the top layers of the polymer solution during regeneration in the coagulation bath.[33] Ichwan and Son have prepared dense RCM from

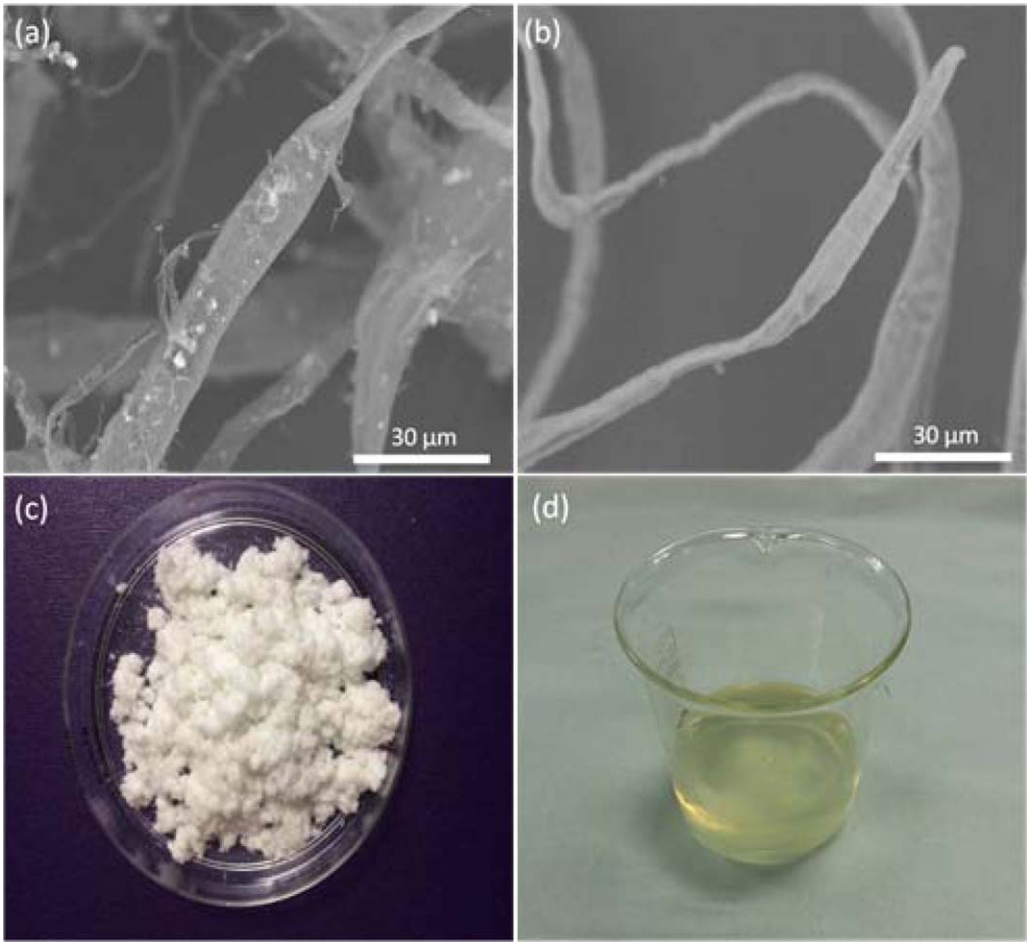

Figure 2. SEM images of (a) RNP-pulp, (b) t-CMF, (c) photograph of cellulose microfiber extracted from recycled newspaper (c), and (d) cellulose dope solution after being dissolved in NaOH/urea aqueous solution and precooled at −15°C. [Color figure can be viewed in the online issue, which is available at wileyonlinelibrary.com.]

N-methylmorpholine-*N*-oxide (NMMO)/water solvent system that possesses dense asymmetric structure with comparable membrane porosity with our study as shown in Table I.[18] Moreover, Biganska and Navard also have prepared RCM by using NMMO/water solvent system but the RCM produced possesses finger-like structure.[33] The formation of finger-like structure is triggered when non-solvent enters into polymer solution faster than the solvent diffuses out. In other words, the finger-like voids are formed when a low viscosity fluid (water) is displacing a more viscous one (molten cellulose dope solution) in the coagulation bath.[33] On the other hand, the formation of dense homogeneous structure was probably due to the intermolecular interactions in cellulose during coagulation with H_2SO_4.[34] Moreover, the dense structure formation was resulted from the nucleation and growth mechanism of the slow solidification process.[35] Ying and co-workers suggested that the changes in mean pore size and pore size distribution may be attributed by the interaction in the polymer side chains during membrane fabrication.[36] It has been reported that the p*Ka* values for cellulosic hydroxyl groups range from 13.4 to 13.7.[37] In the fabrication of the membrane at pH values lower (more acidic) than the p*Ka* of the cellulose polymer, the anionic nature of the cellulose side chains is reduced. Consequently, the electrostatic repulsion among the adjacent chains is reduced. The reduction in electrostatic repulsion promotes a closer packing of the polymer chains and thus, resulted in a substantially denser membrane structure with low mean pore size.[36]

Based on the membrane porosity and membrane mean pore size analysis, prepared RCM with low mean pore size and porosity of 2.48 ± 0.41 nm and $41.03 \pm 2.37\%$, respectively, was obtained. Therefore, the resultant RCM can be considered in the range of ultrafiltration (1 nm to 0.1 μm). It was difficult to observe the pore of RCM from the cross section of scanning micrograph magnification as the pore size was in the range of nanoscale. The resultant RCM pore size in this study was relatively low as compared with the previous studies as shown in the Table I. The differences in mean pore size and the porosity is likely due to different fabrication approach implemented. Feiya and coworkers concluded that the larger pores of the RCM were easily formed with low coagulation concentration than those from the coagulation bath with a higher concentration.[38] In addition, it have been concluded that the RCM coagulated with acidic aqueous solution produces smaller pore size and narrower distribution than those of RCM coagulated with

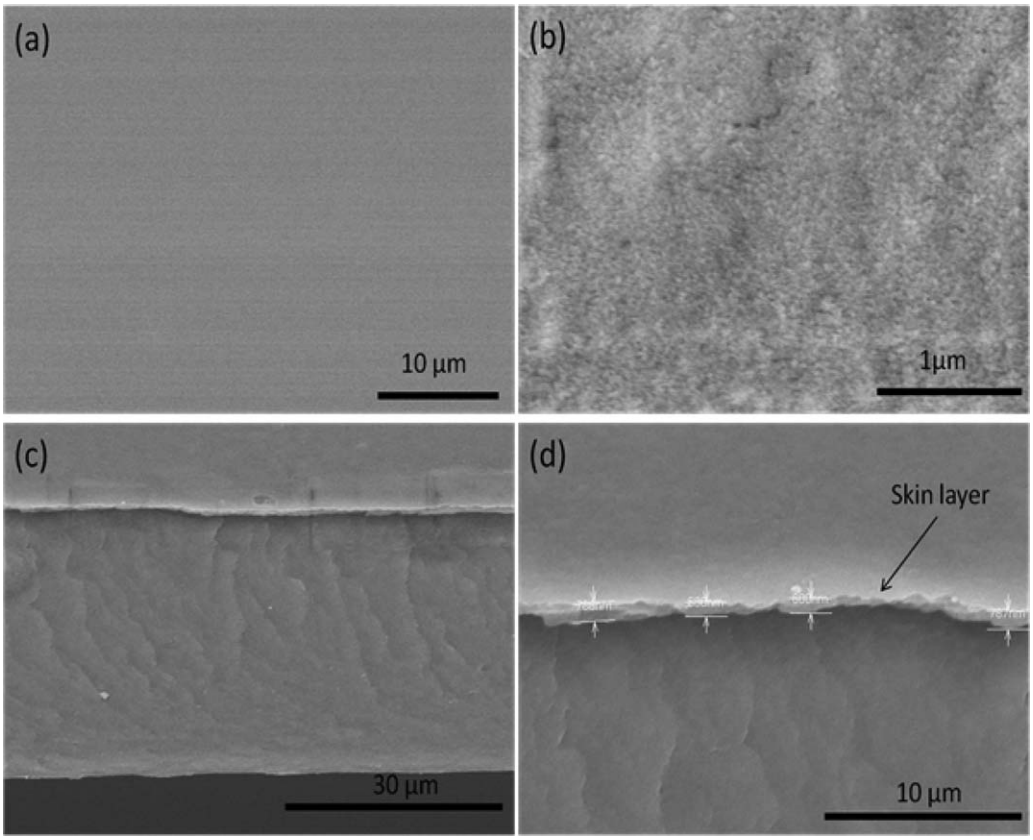

Figure 3. SEM images of the RCM (a), (b) surface and (c), (d) cross section.

pure water and salt aqueous solution, whereas those coagulated with organic coagulant possesses relatively large pore size and wide distribution.[17]

Figure 4(a,b) present the AFM images in 3D view and height view of the surface topography of the RCM, respectively. Contradictory with the SEM image of free surface of RCM in Figure 3(a), a slightly rough surface of the RCM was observed in the AFM images. The difference in surface topography was due to the limitation of scanning micrograph magnification as the AFM technique can only detect surface roughness at nano-scale level. The mean roughness parameter, R_a of 29.53 nm was obtained from the AFM analysis. The R_a value obtained from this study is relatively high as compared to the previous studies as shown in Table II.[18,39] The high in surface roughness is probably due to the prominent formation of nodular with spherical cell that promote compact conformation and irregularities on the membrane surface.[40] Furthermore, based on the previous studies, the surface roughness of the membrane were decreased with the increase in polymer concentration.[41,42] Therefore, the high surface roughness in our study can be justified by the low concentration of cellulose (4 wt %) employed as compared to Ichwan and coworkers (8–11 wt %). TEM image as shown in Figure 4(c) revealed that the formation of the RCM after the regeneration process consisted of compact granular clusters, which indicated the regeneration process would result in dense structure. The results were in agreements with those of recent study reported by Geng and coworkers.[22]

In this study, the RCM was successfully prepared via phase inversion technique. Generally, phase inversion can be described as a demixing process where the initially homogeneous polymer solution is transformed in a controlled manner from a liquid to a solid state. The transformation from cellulose dope solution into thin film membrane was accomplished by immersion precipitation approach where the polymer solution is immersed in a non-solvent coagulation bath (typically water).[44,45] Demixing and precipitation occur due to the exchange of NaOH/urea aqueous solvent system (from cellulose dope solution) and non-solvent (5 wt % H_2SO_4) aqueous solution (from coagulation bath). Mao and co-workers suggested that the membrane formation process is mainly related to the diffusion between non solvent and solvent in the cellulose dope solution.[17] When the rate of non-solvent diffusion into the cast RCM is higher, more pores will emerge. The emerged pore size will continue to grow as long as the non-solvent can diffuse into the growing pore.[46] The diffusion of non-solvent into the growing pore will cause an increase in the cellulose concentration of the cellulose-rich phase surrounding the pore.[43,46] When the surrounding cellulose-rich phase enters the solidification phase, it will spontaneously stops the growth of the pores.[17,18] The solidification phase is reached when the viscosity of the cellulose polymer (cellulose-rich phase) was increased which limits the motion of the cellulose chain and thus solidifies the membrane. Therefore, the solidification of the polymer membrane is the major factor in determining pore size. In addition, when the affinity between

Table I. Summary of the Properties and Pure Water Flux of RCM

Cellulose sources	Solvent aqueous system	Coagulation bath	Structure properties	Mean pore size (nm)	Porosity (%)	Permeability (mL h^{-1} m^{-2} $mmHg^{-1}$)	Reference
RNP	7 wt % NaOH/12 wt % urea	5% H_2SO_4 at 25°C	Homogeneous symmetric dense structure	2.48 ± 0.41	41.03 ± 2.37	0.47 ± 0.02	This work
Cotton linter	7.5 wt % NaOH/11 wt % urea	5% H_2SO_4	Homogeneous mesh network structure	30.6	87	41.50	17
Cellulose carbamate	7 wt % NaOH/1.6 wt % ZnO	3 wt % H_2SO_4	Homogeneous mesh network structure	115-624	87-91	10.93-23.66	36
Cotton linter	6 wt % NaOH/4 wt % urea	$CaCl_2$ aqueous solution + 3 wt % HCl	Homogeneous mesh network structure	120-140	84-86	66.5-82.9	37
Softwood pulp	NMMO/water mixture	H_2O	Dense asymmetric structure	13.4-20.2	24-41	28.17-47.67	18
Cellulose pulp	NMMO/water mixture	H_2O	Finger-like structure	-	-	-	33
Bacteria cellulose	4 wt % NaOH/ 3 wt % urea	5 wt % CaCl + 1 wt % HCl	Dense porous structure	1.26	-	-	38
Cotton pulp	Ionic liquid (1-butyl-3-methylimidazolium chloride)	H_2O	Homogeneous nonporous surface	-	-	-	39

solvent and non-solvent is relatively low, the diffusion rate will slow down and allow nuclei to grow homogenously to yield denser and smaller pore size of membrane structure as shown in Figure 3.[1818] Low mutual affinity between solvent and non-solvent is due to the increase in the cellulose concentration of the cellulose rich phase.[46]

FT-IR Analysis

The chemical structures of RNP-pulp, t-CMF, and RCM were analyzed using FTIR analysis in the range of 4000–650 cm^{-1} as shown in Figure 5. It was observed that all samples exhibited identical FTIR spectrum with slightly shifted absorption band. The absorption band at 3287 cm^{-1} for RCM clearly broadened as compared to those of t-CMF and RNP-pulp. Previous studies suggested that the broadened band was attributed to intra- and inter-molecular of hydrogen bond, respectively.[21,47] As t-CMF was dissolved in NaOH/urea/H_2O pre-cooled at −15°C, the intra- and intermolecular hydrogen bonds of cellulose were broken. Thus, the rearrangement of hydrogen bonding of the RCM occurred during the coagulation in 5% of H_2SO_4. In addition, the FTIR spectrum for RNP-pulp showed the presence of lignin characteristic at 1505 cm^{-1} absorption band, indicating that C=C stretching of aromatic ring was present in lignin.[48,49] However, this peak was absent in t-CMF and RCM spectrum. This indicated that the lignin had been removed after being treated using acidified $NaClO_2$.

The FTIR analysis revealed that the produced RCM showed the characteristic peaks of cellulose II with evident main absorption peak shift.[50,51] The band at 891 cm^{-1} (cellulose II) assigned to C—O—C stretching at β-linked glucose of cellulose was shifted from 897 cm^{-1} (cellulose I) in t-CMF and RNP-pulp.[52–54] Similar observation can also be found in previous study.[51] In addition, the transformation from cellulose I to cellulose II was observed at band 1419 cm^{-1} (cellulose II). This peak was assigned to CH_2 symmetry bending, shifted from 1428 cm^{-1} (cellulose I) in t-CMF and RNP-pulp with decrease in absorption peak. The alteration of its crystalline conformation from cellulose I to II can be explained by the fact that the presence of NaOH creates significant ion-pair interactions, which reduce the strong self-associated character of water, favoring the establishment of hydrogen bonds between urea molecules and cellulose chains.[34] These new intermolecular interactions bring the cellulose into the aqueous solution and, spontaneously modify its crystalline conformation from cellulose I to II during regeneration in the coagulation bath. The summary of main absorbance peaks of interest of this study is listed in Table III.

Crystallinity Study

The XRD patterns of RNP-pulp, t-CMF and RCM are shown in Figure 6. It was seen that both RNP-pulp and t-CMF displayed a typical crystal lattice of cellulose I with main diffraction at $2\theta = 16.5$°C (110 crystal plane) and 22.5° (200 crystal plane) peak pattern.[55,56] Moreover, there were two peaks observed at

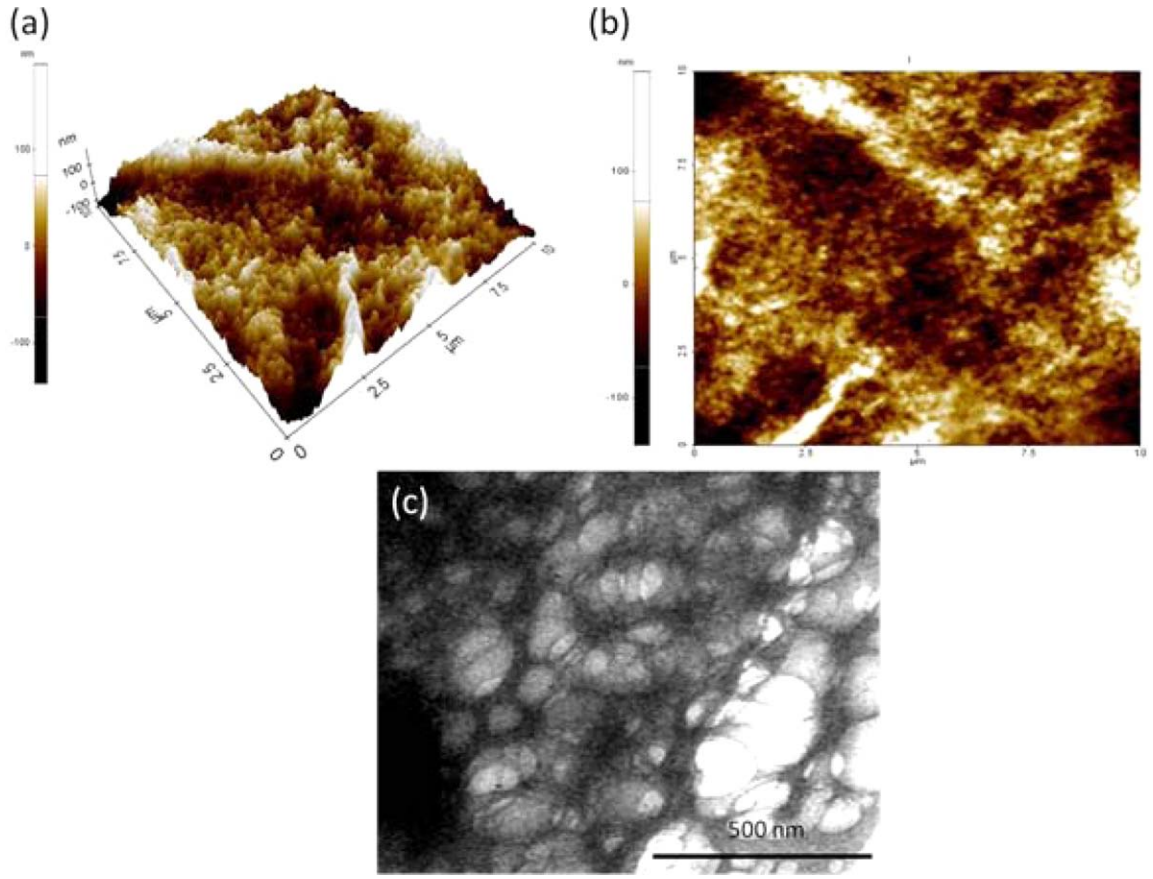

Figure 4. AFM images (a) 3D view and (b) height view, and (c) TEM image of RCM. [Color figure can be viewed in the online issue, which is available at wileyonlinelibrary.com.]

$2\theta = 11.6°$ and 21.6° corresponding to the (110 crystal plane) and (200 crystal plane), respectively. These peaks were attributed to the typical crystal lattice of cellulose II in RCM.[3] Similar XRD pattern was also observed in previous studies.[18,23,57] The results revealed that the crystal lattice of cellulose in RCM produced from NaOH/urea aqueous solution transformed from cellulose I into cellulose II. Furthermore, the transformation of cellulose I to cellulose II was in good aggreement with the FTIR analysis.

The intensity of XRD peak for t-CMF became sharper than RNP-pulp, which indicated the increase in the degree of crystallinity. The higher crystallinity index of t-CMF (93.6%) than RNP-pulp (87.0%) was attributed to the more compact and ordered crystalline structure after having treated by NaOH and $NaClO_2$. However, RCM exhibited the lowest crystallinity index (42.2%) as compared to the RNP-pulp and t-CMF. The decrease in crystallinity index was due to the rearrangement of the cellulose macromolecules during dissolution and regeneration.[3] The dissolution of t-CMF in NaOH/urea aqueous solution had destroyed its original crystalline form by rapidly destroying the

Table II. Contact Angle and Surface Roughness Comparison with Previous Studies

Cellulose source	Contact angle/°	Surface roughness (R_a)/nm	Reference
RNP	55.68 ± 3.83	29.53	This work
Softwood pulp	28–40	2.17–6.31	18
Commercial RCM	26 ± 3	18.5 ± 0.6	39

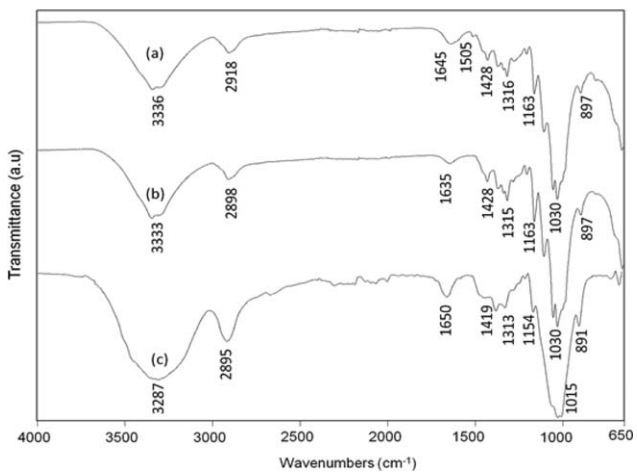

Figure 5. FTIR spectrum of (a) RNP-pulp, (b) t-CMF, and (c) RCM.

Table III. FT-IR Absorption Band for Functional Group of RNP, t-CMF, and RCM

	Peak frequency (cm^{-1})		
Peak assignment	RNP-pulp	t-CMF	RCM
O—H stretching	3336	3333	3336
C—H stretching	2918	2898	2895
O—H bending	1645	1635	1650
C=C stretching of aromatic ring	1505	-	-
CH_2 symmetric bending	1428	1428	1419
C—H bending	1370	1375	1369
CH_2 wagging	1316	1315	1313
C—O anti-symmetric stretching	1163	1163	1154
C—O and C—C stretching	1104	1105	1105
C—O—C stretching	1053	1054	-
C—O and C—C stretching	1030	1030	1015
C—O—C stretching	897	897	891

inter- and intramolecular hydrogen bonds between the cellulose molecules.[26,58]

Thermal Stability Study

Thermal stability analysis was conducted to compare the thermal stability of prepared RCM with t-CMF and RNP-pulp. The TGA and DTG curves of RCM, together with t-CMF and RNP-pulp sample are presented in Figure 7. The thermal degradation data ($T_{5\%}$, $T_{20\%}$, $T_{50\%}$, and T_{max}) as well as residual weight at 600°C are listed in Table IV. Figure 7 shows that all samples had initial weight loss in the temperature range between 29°C to 110°C, which indicated the evaporation of the moisture on the surfaces of the samples.[48,53] The chemisorbed water or the intermolecularly H-bonded water existed in the sample as confirmed by FTIR of this peaks assignment, located at 1645 or 1635 cm^{-1}.

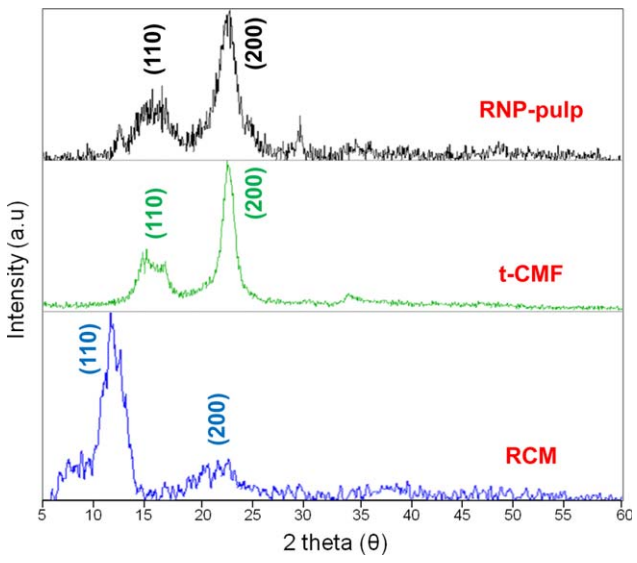

Figure 6. XRD diffractogram of RNP-pulp, t-CMF, and RCM. [Color figure can be viewed in the online issue, which is available at wileyonlinelibrary.com.]

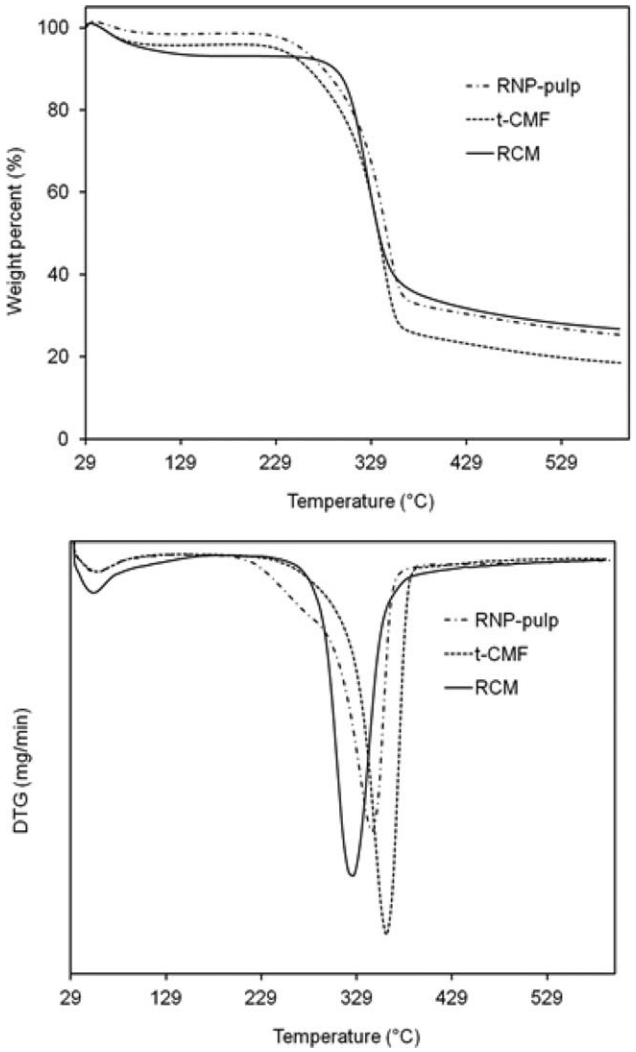

Figure 7. TG and DTG curve of (a) t-CMF, (b) RNP-Pulp, and (c) RCM.

The TGA and DTG curves in Figure 7 show that all samples followed almost identical degradation mechanism since there were very small significant differences in $T_{5\%}$, $T_{20\%}$, and $T_{50\%}$, as shown in Table IV. However, the DTG curves revealed that t-CMF exhibited the highest thermal stability since the maximum rate of degradation occurred at T_{max} of 360.8°C, followed by RNP-pulp and RCM at T_{max} of 346.4°C and 326.3°C,

Table IV. Thermal Stability Data of RNP-Pulp, t-CMF, and RCM

Samples	$T_{5\%}$ (°C)	$T_{20\%}$ (°C)	$T_{50\%}$ (°C)	DTG peak, T_{max} (°C)	Residue at 600°C (%)
RNP-Pulp	252.9	305.6	340.6	346.4	25.3
t-CMF	233.5	291.5	337.8	360.8	18.5
RCM	263.4	308.9	338.9	326.3	26.8

respectively. Furthermore, sample t-CMF exhibited the lowest in residual percent, at about 18.5%, followed by RNP-pulp and RCM about 25.3% and 26.8%, respectively. It has been reported by previous works that the thermal stability of cellulose fiber will be increased as it undergoes alkalization and bleaching treatment.[31,53,59,60] The improvement in thermal stability after chemical treatment was due to the removal of non-cellulosic materials (hemicelluloses and lignin), which resulted in dense and compact structure, and therefore, increase of the degradation temperature and lowering of the residual percentage. However, it is quite interesting to note that, the resultant RCM exhibited the lowest thermal stability compared to its origin source t-CMF. Previous research has indicated that reduced thermal stability is highly due to the low crystallinity which can accelerate the degradation process.[61]

Hydrophilic Properties

The hydrophilicity property of RCM was studied based on water contact angle (WCA) measurement and WC [eq. (3)]. Previous study suggested that the strong hydrophilic property was attributed to the interaction of hydroxyl group in cellulose with water molecule and led to the surface contact angle, which was observable at surface contact angle below 90°.[18] Furthermore, the WC in the regenerated membrane was related to the membrane hydrophilicity property.[29] Thus, in this study, we were able to prepare RCM with hydrophilicity property with the equilibrium water contact angle and WC value of $55.68 \pm 3.83°$ and $40.95 \pm 2.53\%$, respectively. . In general, cellulose membrane in nature possesses high hydrophilicity. However, as compared to the previous study as shown in the Table II, the prepared RCM exhibit relatively high water contact angle might be due to the high surface roughness as compared to others which at huge extent of adding certain hydrophobicity to the surface of prepared RCM.[62]

Meanwhile, the low water permeability of the prepared RCM was achieved through pure water flux measurement. In general, the pure water flux has a close relationship with hydrophilicity, WC, and the morphological structure of the membrane. Yuan Mao and co-workers suggested that the water permeability are related to porosity and amount of through pore in the membranes.[17] Therefore, as compared to the previous study (Table I), it is worth to note that the low in permeability in this study is due to the low in mean pore size and porosity.[38] Membranes with high hydrophilicity properties and low surface roughness are very crucial in filtration and separation since these lead to a lower fouling tendency.[30,63] The fouling phenomena on the surface of membrane will reduce the performance of membrane, require increased energy expenditure or cleaning frequency.[64]

CONCLUSION

In this study, the utilization of RNP as the cellulose source for the fabrication of RCM was successfully prepared through low cost and environmental friendly process with application of 7 wt % NaOH/12 wt % urea aqueous solution technique. The extraction of the cellulose from RNP through NaOH and $NaClO_2$ pretreatment promoted the production of high crystallinity index of the cellulose microfiber (CMF) with 5–8 μm in width, due to the removal of lignin and other extractives on the surface of the CMF. The regeneration of the cellulose dope solution led to the production of the RCM with the transformation of cellulose structure type I to type II, which have been confirmed by FTIR and XRD analysis. From SEM, AFM, and TEM observation, the resultant membrane was observed exhibiting homogeneous dense symmetric membrane structure which was composed of a skin layer with mean pores size and porosity of 2.48 ± 0.41 nm and $41.03 \pm 2.37\%$. Therefore, the resultant RCM can be considered in the range of ultrafiltration (1 nm to 0.1 μm). The produced RCM possessed a hydrophilic property which the contact angle of surface observed at $55.68 \pm 3.83°$ and WC value of $40.95 \pm 2.53\%$. In general, this work provides a novel process for the manufacture of RCM and fiber from RNP. The findings from this study showed that, RCM has a potential to be applied in ultrafiltration application. This work provided a promising way to prepare RCM with symmetric dense structure and applied a green fabrication approach for the production of the RCM. In addition, this study provides an alternative to paper recycling and possibly address the issue of by-products arising from paper to paper recycling.

ACKNOWLEDGMENTS

The authors thank Universiti Teknologi Malaysia (UTM), Ministry of Higher Education Malaysia (MOHE) and Research University Grant (05H08) for the facilities and financial support.

REFERENCES

1. Liu, E. K.; He, W. Q.; Yan, C. R. *Environ. Res. Lett.* **2014**, *9*, 091001.
2. Rodrigues Filho, G.; Monteiro, D. S.; Meireles, C. D. S.; de Assunção, R. M. N.; Cerqueira, D. A.; Barud, H. S.; Ribeiro, S. J. L.; Messadeq, Y. *Carbohydr. Polym.* **2008**, *73*, 74.
3. Qi, H.; Chang, C.; Zhang, L. *Green Chem.* **2009**, *11*, 177.
4. Schurz, J. *Prog. Polym. Sci.* **1999**, *24*, 481.
5. Ramesh Babu, P.; Gaikar, V. G. *Sep. Purif. Technol.* **2001**, *24*, 23.
6. Dogan, H.; Hilmioglu, N. D. *Vacuum* **2010**, *84*, 1123.
7. Xiong, X.; Duan, J.; Zou, W.; He, X.; Zheng, W. *J. Membr. Sci.* **2010**, *363*, 96.
8. Yang, Q.; Fukuzumi, H.; Saito, T.; Isogai, A.; Zhang, L. *Biomacromolecules* **2011**, *12*, 2766.
9. Singh, N.; Chen, Z.; Tomer, N.; Wickramasinghe, S. R.; Soice, N.; Husson, S. M. *J. Membr. Sci.* **2008**, *311*, 225.
10. Fukuzumi, H.; Saito, T.; Iwata, T.; Kumamoto, Y.; Isogai, A. *Biomacromolecules* **2009**, *10*, 162.
11. Ma, H.; Burger, C.; Hsiao, B. S.; Chu, B. *Biomacromolecules* **2012**, *13*, 180.
12. Zhu, T.; Lin, Y.; Luo, Y.; Hu, X.; Lin, W.; Yu, P.; Huang, C. *Carbohydr. Polym.* **2012**, *87*, 901.
13. Lin, W.-C.; Lien, C.-C.; Yeh, H.-J.; Yu, C.-M.; Hsu, S.-H. *Carbohydr. Polym.* **2013**, *94*, 603.

14. Jayaramudu, J.; Reddy, G. S. M.; Varaprasad, K.; Sadiku, E. R.; Sinha Ray, S.; Varada Rajulu, A. *Carbohydr. Polym.* **2013**, *93*, 622.
15. Yang, Q.; Qi, H.; Lue, A.; Hu, K.; Cheng, G.; Zhang, L. *Carbohydr. Polym.* **2011**, *83*, 1185.
16. Liu, J.; Wang, J.; Bachas, L. G.; Bhattacharyya, D. *Biotechnol. Prog.* **2001**, *17*, 866.
17. Mao, Y.; Zhou, J.; Cai, J.; Zhang, L. *J. Membr. Sci.* **2006**, *279*, 246.
18. Ichwan, M.; Son, T. *J. Appl. Polym. Sci.* **2011**, *124*, 1409.
19. Mahmoudian, S.; Wahit, M. U.; Ismail, A. F.; Yussuf, A. A. *Carbohydr. Polym.* **2012**, *88*, 1251.
20. Liebert, T.; Schiller, F.; Jena, D.- In In Cellulose Solvents: For Analysis, Shaping and Chemical Modification, American Chemical Society: Washington, DC, **2010**; p 3.
21. Luo, X.; Zhang, L. *J. Chromatogr. A* **2010**, *1217*, 5922.
22. Geng, H.; Yuan, Z.; Fan, Q.; Dai, X.; Zhao, Y.; Wang, Z.; Qin, M. *Carbohydr. Polym.* **2014**, *102*, 438.
23. Yang, Q.; Qin, X.; Zhang, L. *Cellulose* **2011**, *18*, 681.
24. Luo, X.; Zhang, L. *J. Hazard. Mater.* **2009**, *171*, 340.
25. Yang, Q.; Lue, A.; Zhang, L. *Compos. Sci. Technol.* **2010**, *70*, 2319.
26. Cai, J.; Zhang, L. *Macromol. Biosci.* **2005**, *5*, 539.
27. Mohamed, M. A.; Salleh, W. N. W.; Jaafar, J.; Asri, S. E. A. M.; Ismail, A. F. *RSC Adv.* **2015**, *5*, 29842.
28. Segal, L.; Creely, J. J.; Martin, A. E.; Conrad, C. M. *Text. Res. J.* **1959**, *29*, 786.
29. Abedini, R.; Mousavi, S. M.; Aminzadeh, R. *Desalination* **2011**, *277*, 40.
30. Hamid, N. A. A.; Ismail, A. F.; Matsuura, T.; Zularisam, A. W.; Lau, W. J.; Yuliwati, E.; Abdullah, M. S. *Desalination* **2011**, *273*, 85.
31. Chen, X.; Yu, J.; Zhang, Z.; Lu, C. *Carbohydr. Polym.* **2011**, *85*, 245.
32. Cai, J.; Zhang, L.; Zhou, J.; Li, H.; Chen, H.; Jin, H. *Macromol. Rapid Commun.* **2004**, *25*, 1558.
33. Biganska, O.; Navard, P. *Cellulose* **2009**, *16*, 179.
34. Zhang, L.; Ruan, D.; Zhou, J. *Ind. Eng. Chem. Res.* **2001**, *40*, 5923.
35. Liu, S.; Zhang, L. *Cellulose* **2009**, *16*, 189.
36. Ying, L.; Zhai, G.; Winata, A. Y.; Kang, E. T.; Neoh, K. G. *J. Colloid Interface Sci.* **2003**, *265*, 396.
37. Saric, S. P.; Schofield, R. K. *Proc. R. Soc. London* **1946**, *185*, 431.
38. Fu, F.; Guo, Y.; Wang, Y.; Tan, Q.; Zhou, J.; Zhang, L. *Cellulose* **2014**, *21*, 2819.
39. Pieracci, J.; Crivello, J. V.; Belfort, G. *J. Membr. Sci.* **1999**, *156*.
40. Khulbe, K. C.; Feng, C. Y.; Matsuura, T. *Synthetic Polymeric Membranes*, **2008**, 47–100.
41. Akbari, A.; Hamadanian, M.; Jabbari, V.; Lehi, A. Y.; Bojaran, M. *Desalin. Water Treat.* **2012**, *46*, 96.
42. Sani, N. A. A.; Lau, W. J.; Ismail, A. F. *Korean J. Chem. Eng.* **2015**, *32*, 743.
43. Strathmann, H.; Kock, K. *Desalination* **1977**, *21*, 241.
44. Lalia, B. S.; Kochkodan, V.; Hashaikeh, R.; Hilal, N. *Desalination* **2013**, *326*, 77.
45. Peng, N.; Widjojo, N.; Sukitpaneenit, P.; Teoh, M. M.; Lipscomb, G. G.; Chung, T. S.; Lai, J. Y. *Prog. Polym. Sci.* **2012**, *37*, 1401.
46. Young, T.-H.; Chen, L.-W. *Desalination* **1995**, *103*, 233.
47. Kondo, T.; Sawatari, C.; Gray, D. G.; Manley, R. S. J.; Gray, D. G. *Macromolecules* **1994**, *27*, 210.
48. Mandal, A.; Chakrabarty, D. *Carbohydr. Polym.* **2011**, *86*, 1291.
49. Samfira, I.; Butnariu, M.; Rodino, S.; Butu, M. *Dig. J. Nanomater. Biostructures* **2013**, *8*, 1679.
50. Oh, S. Y.; Il Yoo, D.; Shin, Y.; Kim, H. C.; Kim, H. Y.; Chung, Y. S.; Park, W. H.; Youk, J. H. *Carbohydr. Res.* **2005**, *340*, 2376.
51. Yue, Y.; Han, G.; Wu, Q. *Bioresources* **2013**, *8*, 6460.
52. Elanthikkal, S.; Gopalakrishnapanicker, U.; Varghese, S.; Guthrie, J. T. *Carbohydr. Polym.* **2010**, *80*, 852.
53. Sonia, A.; Priya Dasan, K. *Carbohydr. Polym.* **2013**, *92*, 668.
54. Mohamad Haafiz, M. K.; Eichhorn, S. J.; Hassan, A.; Jawaid, M. *Carbohydr. Polym.* **2013**, *93*, 628.
55. Bondeson, D.; Mathew, A.; Oksman, K. *Cellulose* **2006**, *13*, 171.
56. Kumar, A.; Negi, Y. S.; Choudhary, V.; Bhardwaj, N. K. *J. Mater. Phys. Chem.* **2014**, *2*, 1.
57. Zhang, X.; Chen, W.; Lin, Z.; Yao, J.; Tan, S. *Synth. React. Inorganic, Met. Nano-Metal Chem.* **2011**, *41*, 997.
58. Zhang, H.; Wu, J.; Zhang, J.; He, J. *Macromolecules* **2005**, *38*, 8272.
59. Bhattacharya, D.; Germinario, L. T.; Winter, W. T. *Carbohydr. Polym.* **2008**, *73*, 371.
60. Morán, J. I.; Alvarez, V. A.; Cyras, V. P.; Vázquez, A. *Cellulose* **2007**, *15*, 149.
61. Poletto, M.; Zattera, A. J.; Forte, M. M. C.; Santana, R. M. C. *Bioresour. Technol.* **2012**, *109*, 148.
62. Yoshimitsu, Z.; Nakajima, A.; Watanabe, T.; Hashimoto, K. *Langmuir* **2002**, *18*, 5818.
63. Damodar, R. A.; You, S.-J.; Chou, H.-H. *J. Hazard. Mater.* **2009**, *172*, 1321.
64. Miller, D. J.; Kasemset, S.; Wang, L.; Paul, D. R.; Freeman, B. D. *J. Membr. Sci.* **2014**, *452*, 171.